Contents lists available at Science-Gate

International Journal of Advanced and Applied Sciences

Journal homepage: http://www.science-gate.com/IJAAS.html

Simulation of FSO systems using VPI transmission maker

Wansu Lim *

Kumoh National Institute of Technology, Gumi, South Korea

A R T I C L E I N F O

Article history:
Received 27 December 2015
Received in revised form
25 January 2016
Accepted 26 January 2016

Keywords:
Free space optical (FSO) systems
Phase noise
Intermodulation distortion
VPI transmission Maker

A B S T R A C T

In this paper, FSO systems have been simulated using VPI simulator. We first present the simulation environment with the description of VPI components and VPI models for FSO systems considering the effect of the phase noise and intermodulation distortion. As a simulation result, we investigate the performance evaluation according to various parameters.

1. Introduction

The invention of optical fibers, enabling the development of low loss and huge bandwidth communications, has opened a high speed multimedia communication era. As a result, a variety of optical networks have been introduced, which are categorized according to topologies, applications and even communication techniques. In particular, the FSO systems are well-known for covering access network by connecting metropolitan and backbone networks, managing metro-gaps, continuing various services from the backbone network (Zhu et al., 2015; Lee and Hwang, 2015). This network is especially advantageous of reducing the cost, simple structure, high security and no need to dig for installation of FSO systems.

In (Lim et al., 2012, 2009), we investigated the analytical performance of the FSO systems. As aforementioned, the analysis can be used to evaluate the exact performance or provide a closed form for the error rate under given channel conditions. It is not always possible, however, to get a closed form equation from the analysis especially for the turbulence channels. In an alternative, we can rely on the simulation of a specific system to conform the analytical results, understand the characteristics of the channel or evaluate the system performance. We present the simulation methods and results of FSO systems under turbulence channels considering the effect of phase noise and intermodulation distortion (IMD) using VPI transmission Maker (The VPI transmission Maker function site).

The transmitted signal undergoes the degradation factors such as phase noise and intermodulation distortion under atmospheric turbulence channels. First, the transmitted signal undergoes the effect of phase noise according to the linewidth of a laser diode in transmitter. Phase noise is the frequency domain representation of rapid, short-term, random fluctuations in the phase of a waveform, caused by time domain instabilities (jitter). Generally speaking radio frequency engineers speak of phase noise of an oscillator, whereas digital system engineers work with the jitter of a clock. Second, IMD is the unwanted amplitude modulation of signals containing two or more different frequencies, each component modulating other components, in a system with nonlinearities. This will form additional signals at frequencies that are not, in general, at harmonic frequencies (integer multiples) of either, but instead often at sum and difference frequencies of the original frequencies. IMD is caused by non-linear behavior of the signal processing being used. The theoretical outcome of these non-linearities can be calculated by conducting a Volterra series of the characteristic, while the usual approximation of those non-linearities is obtained by conducting a Taylor series.

In order to simulate the FSO systems, we use the block diagram shown in Fig. 1. As we can see in the figure, the overall system is partitioned into three parts. The first is the data generation and signal modulation part where the source data is modulated corresponding to the optical modulation methods. The second is the atmospheric turbulence channel part which generates the channel noise of the fading channels with the scintillation effect. The third is the signal demodulation and detection part where the received signals are demodulated and the transmitted signals are recovered by a photo detector.

* Corresponding Author.
Email Address: wansu.lim@kumoh.ac.kr

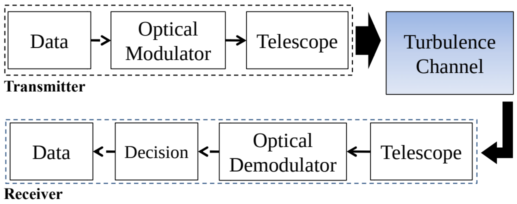

Fig. 1: Conceptual block diagram of the FSO system for simulations under turbulence channels

In the modulation part, the signal is modulated by a Mach-Zehnder modulator. The data stream, modulating the continuous wave laser source, is generated using an NRZ shaped pulse train (module NRZCoder) with a user-defined rise time of the pulses (module RiseTimeAdjust). The modulated and filtered signals are transmitted through turbulence fading channels. The received signals are equalized to compensate the distortions caused by the fading attenuation, and then demodulated. The BER is calculated by the exact moment generation function of the received bits. The more detailed explanations about the individual parts are given in the following sections.

2. Simulation considering the effect of Phase Noise

We describe the system operation to provide and confirm the basic system model. The basic blocks such as the transmitter part, the channel part, the receiver part are used in the simulations under fading channels. Further, the operation of the blocks is also retained. Therefore, we can conduct the proper operation of the basic blocks by observing the BER performance according to the average SNR under turbulence channels. With this object in mind, in this section, we express the simulation methods and the results of the FSO system considering the effect of the phase noise from the laser diode under turbulence channels.

Fig. 2 shows the overall simulation model of the FSO system under turbulence channels by using VPI optical system simulator. In the simulation, we assume the perfect estimation of the received SNR because the simulation is mainly intended to verify the effect of the phase noise. As shown in Fig. 2, the system is consisted of three parts: the transmitter part, the turbulence channel part, the receiver part.

The transmitter part is composed of the laser diode, the bit generator, the line coder, the filter and the Mach-Zehnder modulator as shown in Fig. 3. The laser diode models a laser producing a continuous wave (CW) optical signal. The laser has a side mode, intensity noise, wavelength drift with temperature and linewidth.

The module produces a time dependent field $E(t)$ describing the radiation of a CW laser with the specified power, frequency, linewidth and polarization. We use a pseudo random binary sequence (PRBS) for data generation. The PRBS is usually required when modeling the information source in simulations of digital communication systems. The binary sequence can be generated with the use of a random number generator, or, alternatively, can be directly specified by the user or read from a specified file. The PRBS module produces a sequence of N bits with the numbers m and n of zero bits preceding and succeeding the generated bit sequence of length N-m-n as shown in Fig. 4.

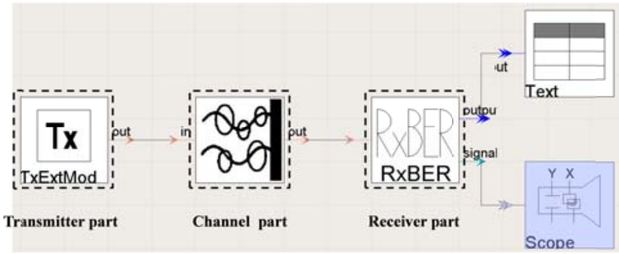

Fig. 2: VPI model for FSO systems.

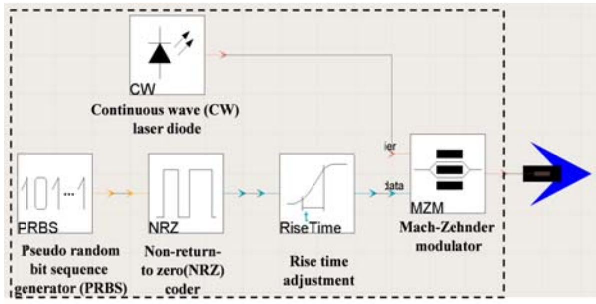

Fig. 3: Transmitter part of VPI model for FSO systems

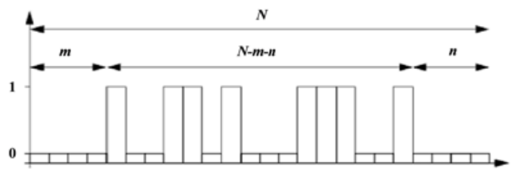

Fig. 4: A sequence of N bits contains m preceding and n succeeding zero bits

The NRZ coder module also generates a sampled, NRZ (Non return to zero) coded signal defined by a train of bits at its input. A NRZ pulse has a single value over the entire bit length, i.e., the “1” is coded by a high level with non-zero amplitude and the “0” by a low level with zero amplitude. The Rise Time module is a Gaussian filter that transforms, for example, rectangular electrical input pulses into smoother output pulses with a user-defined rise-time. Its effect is to band-limit the modulated optical signal, which is required to avoid numerical artifacts when resampling to higher sample rates. In Mach-Zehnder modulator, changing the electric field on the phase modulating path determines whether the two beams interfere constructively or destructively at the output, and thereby control the amplitude or intensity of the exiting light. In the turbulence channel part, we can control the propagation length, the scintillation strength, wavelength, launch waist and the receiver aperture diameter.

The receiver part outputs both the detected electrical signal waveform and the evaluated system performance metrics. It represents a full standard receiver model for intensity modulated direct detection systems, including all components required for signal detection and estimation of error probability. The structure of receiver part consists of a polarization filter, PIN photodetector, arbitrary postdetection low-pass filter and clock recovery as shown in Fig. 5.

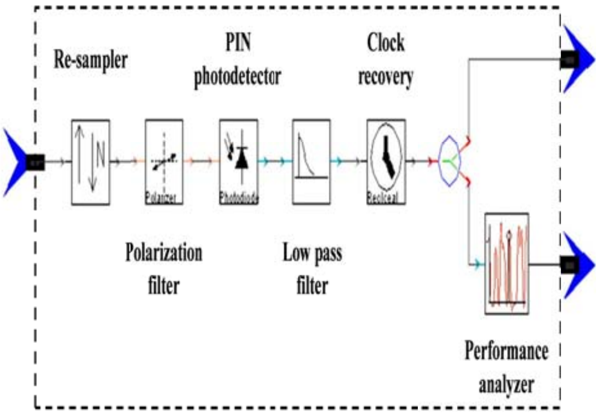

Fig. 5: Internal structure of the receiver part

It also supports to estimate BER, Q-factor and effective Q-factor, in an intensity modulated direct detection optical transmission system. The module estimates the increase in received optical power (ROP) that is required to achieve the prescribed BER. Either deterministic or stochastic approaches can be selected for BER estimation. When the deterministic approach is used, the BER is found from the exact moment generation function of the received bits, which is calculated from the statistical properties of the optical, thermal and shot noises. The calculation algorithm takes into account the influence of an arbitrary spectral shape of the optical noise, resulting from an external optical filtering and arbitrary states of polarization of the signal and noise due to PMD and PDL. When the stochastic approach is used, it is assumed that an optical signal mixed with optical noise has 2 statistics after detection. Four-wave mixing (FWM) noise, post-detection thermal noise, shot noise of PIN detector and intersymbol interference (ISI) can also be taken into account. Gaussian approximation of signal statistics can be used for both the deterministic and stochastic approaches. In Fig. 6, we present the example for the shape of bit sequences in each component (bit generator, MZM and photodetector) as shown in Figs. 2 and 3.

Fig. 6 represents the comparison between the numerical results and the VPI simulation results. When the scintillation strength is weak, the simulation results almost coincide the numerical results, but when the scintillation strength is strong, the simulation results slightly differ the numerical result. For example, at a given SNR of 40 dB in a laser linewidth of 624 MHz, the result of the simulation is almost 1.4 times bigger than that of the numerical analysis under the strong scintillation environment, but the result of the simulation is almost 1.17 times bigger than that of the numerical analysis under the weak scintillation environment. This is because the effect of the scintillation is bigger than that of phase noise under the strong scintillation environment. We also confirm that the simulation results are well match in the relative high average SNR range.

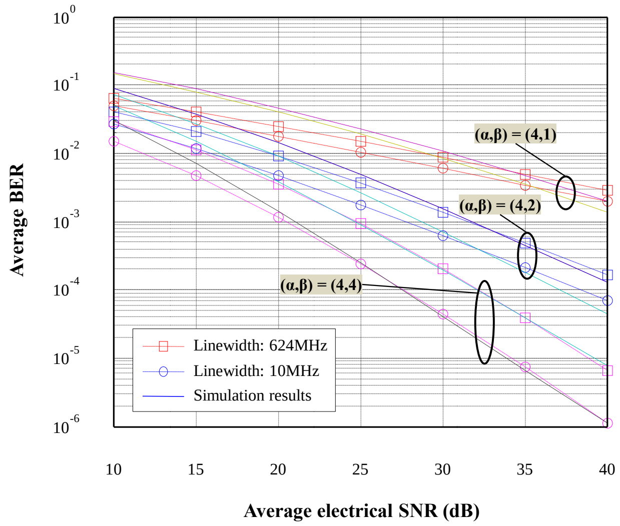

Fig. 6: The performance comparison between simulation results using VPI and numerical analysis results

3. Simulation considering the effect of Intermodulation Distortion

We present the computer simulation using VPI optical system simulator in order to verity the numerical results about the performance evaluation considering the effect of intermodulation distortion. Fig. 7 shows FSO system model including two input RF sinusoidal signals and the SNDR calculation part. Other components are the same with the previous section. In this model, we simulate the received signal power, IM3 power and SNDR according to changing the input RF signal power under the log-normal turbulence channel.

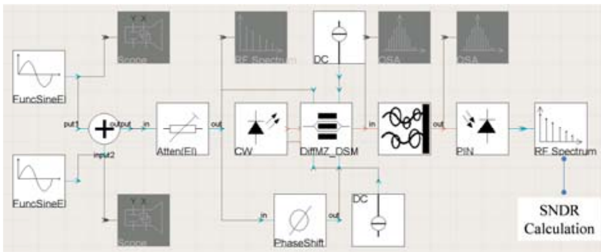

Fig. 7: VPI model for FSO systems to investigate the effect of intermodulation distortion

After passing the photodetector in receiver, we can confirm the intermodulation distortion terms including IM3 as shown in Fig. 8 using RF Spectrum. In the SNDR calculation part as shown in Fig. 9, we first calculate the received signal power and the third order intermodulation distortion (IM3) power, and then we obtain the SNDR using the two power values. For calculation the power of the received signal and IM3, we first use the bandpass filter to extract the received signal and IM3 terms, and then we measure the power using the PowerMeter. Furthermore, we present two examples.

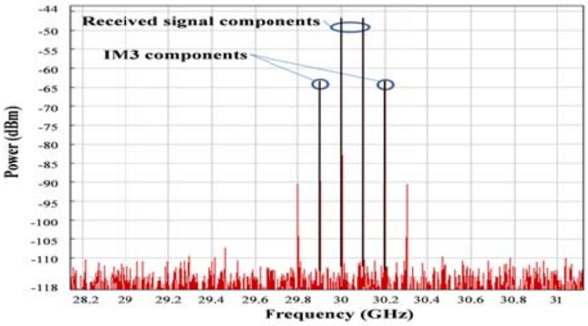

Fig. 8: RF spectrum of the received signal and IM3 components after passing the photodetector

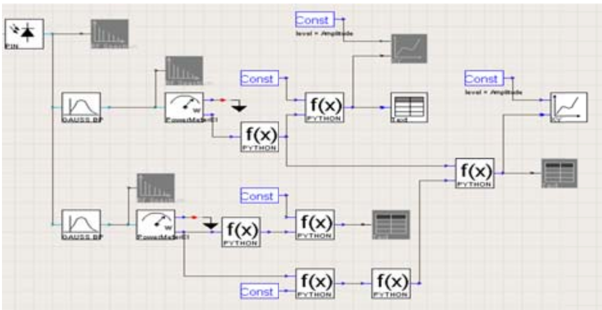

Fig. 9: Block diagram for the calculation of the received signal power and the SNDR

Fig. 10 is about signal transformation processes in frequency domain considering two tone signals with 30 GHz and 30.01 GHz in a transmitter, an optical spectrum after DD-MZM and an RF spectrum after photodector in a receiver.

Fig. 11 represents the comparison between the numerical results and the simulation results in terms of the received signal power, the IM3 power and SNDR. As illustrated in Fig. 11, we verify the correction of the derived numerical analysis through the well matching between the result of simulation and these of analysis. Moreover, we confirm that simulation also has a inflection point due to the effect of the IM3. Thus, SNDR decreases after the some value of the input RF signal power as shown in Figs 11. This is because the IM3 power increase by the cube of input RF signal power, but the received signal power is proportional to the input RF signal power. We also check that the slop of the IM3 is larger than that of the received. As a result, the maximum SNDR is almost 42 dB as a given input RF power of 10 dBm under the log-normal channel.

4. Concluding remarks

We investigate the FSO systems performance considering two kinds of the degradation factors, phase noise and intermodulation distortion (IM3) under various turbulence channel conditions. This is because phase noise is one of the practical and decisive factors in high-quality services that require high SNR and IM3 terms are the most severe compared with the other intermodulation distortion terms because they are too close to the fundamental frequency component and their powers increase faster than the fundamental as shown in Fig. 11. For the simulation, we use VPI transmission Maker Cable Access of VPI photonics. We employ the external modulation with Mach-Zehnder modulator to increase the system performance as shown in Fig. 2 and 10. In order to reflect the characteristics of the turbulence channel, we use the probability density function with the log-normal distribution. Moreover, VPI well support launch waist, receiver aperture and propagation length and scintillation strength.

In the simulation for the effect of the phase noise, the simulator was set with the wavelength of 1550 nm, the data rate of 1 Gbps and the photodetector of PIN. For the simulation of the effect of the IM3, we set the fundamental frequency of 30 GHz and 30.01 GHz. From the simulation results, we observe the following things.

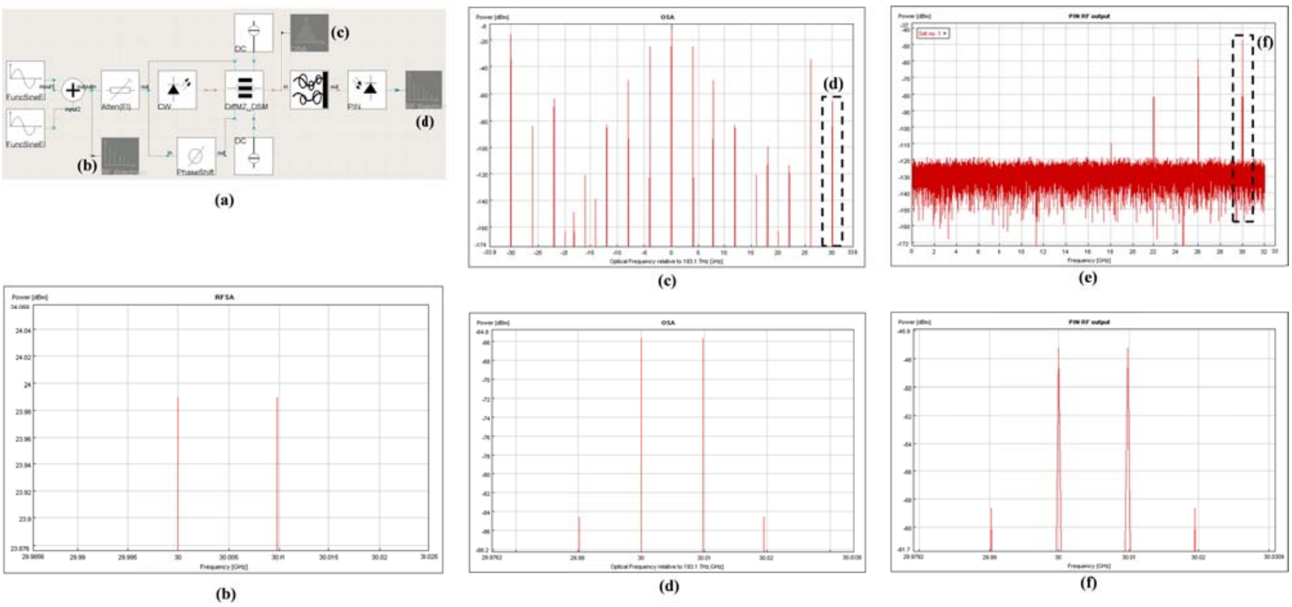

Fig. 10: (a) VPI model and signal transformation processes in frequency domain (b) two tone (30, 30.01 GHz) generation in transmitter, (c) optical spectrum after MZM, (d) some part of (c), (e) RF spectrum after photodetector and (f) some part of (e)

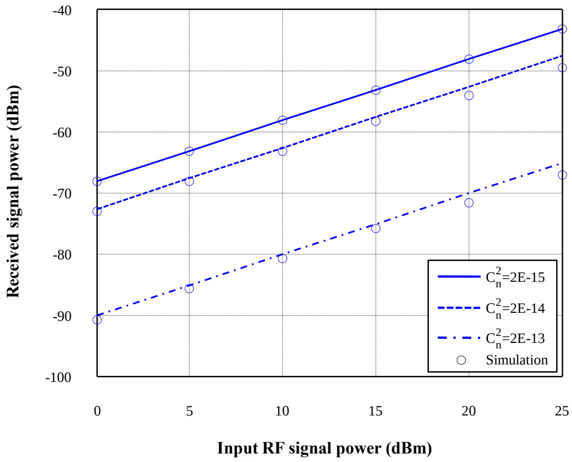

(a)

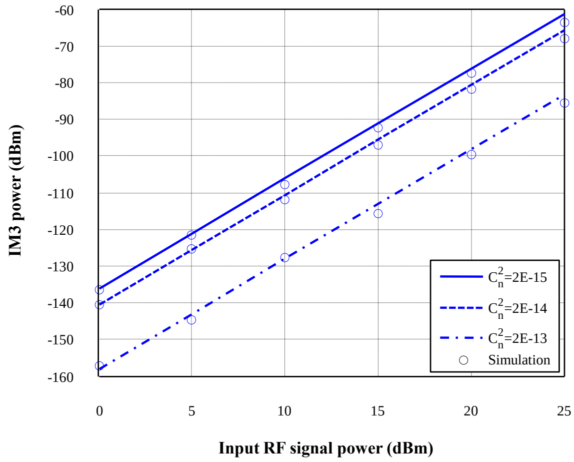

(b)

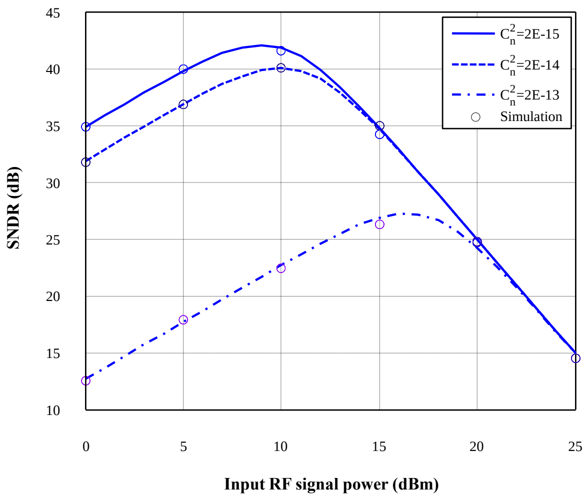

(c)

Fig. 11: (a) The received signal power comparison between simulation results using VPI and numerical analysis results, (b) IM3 power comparison between simulation results using VPI and numerical analysis results, and (c) SNDR comparison between simulation results using VPI and numerical analysis results

First, the trend of the average BER of the four responsivities is very similar to irrelevant to the two kind of linewidth, 10 MHz and 624 MHz. The average BER increases as the propagation length increase. For example, the average BER with propagation length of 1000 m is almost 24.14 dB better than that with 1250 m.

Second, we compare the numerical analysis results considering the effect of the phase with the VPI simulation results. As a result, we confirm that two results are well matched under turbulence channels.

Third, we simulate the received signal power, the IM3 power and the SNDR as a function of the propagation length with three different the scintillation strength $(C_n^2 = 4 \times 10^{-14}, 6 \times 10^{-14}, and 8 \times 10^{-14})$. As a results, we confirm that the the received signal power, the IM3 power and the SNDR with $C_n^2 = 4 \times 10^{-14}$ is almost 4.6 dBm, 3.2 dBm and 4.4 dB better that with $C_n^2 = 8 \times 10^{-14}$ at a given the propagation length of 1500 m, respectively.

Fourth, we simulate the received signal power and the IM3 power as a function of the input RF signal power with three different responsivities (0.4, 0.6 and 0.8). As a results, we confirm that the received signal power and the IM3 power with the responsivity of 0.8 is almost 2.7 dBm and 4.86 dBm better that with the responsivity of 0.4 at a given the input RF signal power of 10 dBm, respectively.

Sixth, we compare the numerical analysis results considering the effect of the IM3 with the VPI simulation results. As a result, we confirm that two results are well matched under turbulence channels.

Acknowledgment

This research was supported by the MSIP (Ministry of Science, ICT and Future Planning), Korea, under the C-ITRC (Convergence Information Technology Research Center) (IITP-2015-H8601-15-1011) supervised by the IITP (Institute for Information and communications Technology Promotion).

References

Lee JH and Hwang SH (2015). Selection diversity-aided subcarrier intensity modulation/spatial modulation for free-space optical communication. Optoelectronics, IET, 9(2): 116-124.

Lim W, Ch, TS, Yun C, Kourtessis P, Kim K and Yang YM (2012). Analytical time-domain model for radio over free space optical (RoFSO) systems considering the scintillation effect. Aerospace and Electronic Systems, IEEE Transactions on, 48(2): 1759-1763.

Lim W, Yun C and Kim K (2009). BER performance analysis of radio over free-space optical systems considering laser phase noise under Gamma-Gamma turbulence channels. Optics express, 17(6): 4479-4484.

Yang L, Cheng J and Holzman JF (2015). Maximum Likelihood Estimation of the Lognormal-Rician FSO Channel Model. Photonics Technology Letters, IEEE, 27(15): 1656-1659.

Zhu B, Cheng J and Wu L (2015). A Distance-Dependent Free-Space Optical Cooperative Communication System. IEEE COMMUNICATIONS LETTERS, 19(6), 969-972.